Available online at www.sciencedirect.com
SCIENCE DIRECT®
Journal of Crystal Growth 252 (2003) 202–207
JOURNAL OF CRYSTAL GROWTH
www.elsevier.com/locate/jcrysgro

# (Ga,Mn,N) compounds growth with mass-analyzed low energy dual ion beam deposition

Fuqiang Zhang[a,b,*], NuoFu Chen[a,b], Xianglin Liu[a], Zhikai Liu[a], Shaoyan Yang[a], Chunlin Chai[a]

[a] *Key Laboratory of Semiconductor Materials Science, Institute of Semiconductor, Chinese Academy of Sciences, P.O. Box 912, Beijing 100083, People's Republic of China*
[b] *National Microgravity Laboratory of Chinese Academy of Sciences, People's Republic of China*

Received 28 November 2002; accepted 19 December 2002
Communicated by R. Kern

**Abstract**

The (Ga,Mn,N) samples were grown by the implantation of low-energy Mn ions into $GaN/Al_2O_3$ substrate at different elevated substrate temperatures with mass-analyzed low-energy dual ion beam deposition system. Auger electron spectroscopy depth profile of samples grown at different substrate temperatures indicates that the Mn ions reach deeper in samples with higher substrate temperatures. Clear X-ray diffraction peak from (Ga,Mn)N is observed in samples grown at the higher substrate temperature. It indicates that under optimized substrate temperature and annealing conditions the solid solution (Ga,Mn)N phase in samples was formed with the same lattice structure as GaN and different lattice constant.
© 2003 Elsevier Science B.V. All rights reserved.

*PACS:* 81.05.Ea; 81.05.Zx; 81.15.Hi; 75.50.Pp; 61.82.Fk

*Keywords:* A1. X-ray diffraction; A3. Ion beam epitaxy; B2. Semiconducting III–V materials

## 1. Introduction

Diluted magnetic semiconductors (DMSs), also called semimagnetic semiconductors, have been studied for decades. The most extensively studied and most thoroughly understood materials of DMSs are III–V based DMSs. III–V based DMSs have been one of the most attracting subjects because of their low temperature ferromagnetism and the important potential applications in microelectronic and optoelectronic fields [1–5]. III–V based DMSs have demonstrated unique phenomena such as field-effect control of ferromagnetism [6,7], efficient spin injection to produce circularly polarized light [6,8,9], and spin-dependent resonant tunneling [4,6]. But the Curie temperature of DMSs is not high enough heretofore. In order to obtain breakthroughs in applications, DMSs

*Corresponding author. Key Laboratory of Semiconductor Materials Science, Institute of Semiconductor, Chinese Academy of Sciences, P.O. Box 912, Beijing 100083, People's Republic of China. Tel.: +86-10-82304627; fax: +86-10-82304469.
*E-mail address:* fqzh@red.semi.ac.cn (F. Zhang).

0022-0248/03/$ - see front matter © 2003 Elsevier Science B.V. All rights reserved.
doi:10.1016/S0022-0248(02)02515-0

should exhibit ferromagnetism above room temperature.

GaN-based DMSs are quite promising for various spin-controlled and photonic devices because of the wide gap corresponding to visible light [10]. And according to a theoretical model considering ferromagnetic behavior of various DMSs [11,12], the Curie temperature of wide band gap semiconductors based DMSs may be above those of GaMnAs (110 K) and InMnAs (<35 K) [13,14]. In particular, GaMnN with ~5% Mn and high hole concentrations is predicted to have a Curie temperature above room temperature [12,14]. If GaN-based DMS is prepared, magnetic phenomena can be introduced into the GaN-based optical and electrical devices.

In order to obtain a heavy doping of Mn in GaN, a highly nonequilibrium growth process is necessary [10]. One of the growth methods is the high-energy $Mn^+$ implantation whose evident advantage is that the growth cost is low. But the implanted high-energy Mn ions will seriously destroy the crystal structure which is impossible to restore by post-annealing, and the formation of secondary phase is inevitable [15]. So in order to overcome the disadvantages of high-energy ions implantation, two methods are adopted. One is the application of the low-energy ions, which can weaken the damage to crystal structure, and the other is the application of the elevated substrate temperature [14], which helps to restore the crystal structure during the process of growth and can make the Mn ions reach deeper in samples. It is expected to acquire excellent materials by these two measures.

In this paper (Ga,Mn,N) samples were grown by the implantation of low-energy Mn ions into unintentionally doped n-type GaN/$Al_2O_3$ substrate at different elevated substrate temperatures with mass-analyzed low-energy dual ion beam deposition system. Under optimized substrate temperature and annealing conditions, the solid solution (Ga,Mn)N phase in samples was found with the same lattice structure as GaN and different lattice constants.

## 2. Material preparation

The GaN samples were grown by metal organic chemical vapor deposition on sapphire substrates. All GaN/$Al_2O_3$ substrates were cleaned before growth. (Ga,Mn,N) samples were prepared by mass-analyzed low energy dual ion beam deposition system. One of its advantages is that there are magneto-mass filters in this system with which the manganese can be purified as pure as isotope. So Mn did not need to be etched and cleaned before growth.

Firstly, in order to remove the adsorbed impurities on the surface of GaN/$Al_2O_3$ substrate, the substrate was bombarded by Argon ions for 10 min. Secondly, the manganese ions with energy of 1 keV were uniformly implanted into (0 0 0 1) oriented GaN/$Al_2O_3$ substrates in the depth of about 60 nm at different substrate temperatures. The dose of manganese ions was about $2.5 \times 10^{14}/cm^2$. During growth, GaN/$Al_2O_3$ substrates were heated to different temperatures. The substrate temperature of sample 1 was 200°C. Those of samples 2 and 3 were 400°C. Thirdly, the manganese ions with energy of 100 eV were deposited on the surface of wafers with the dose of about $1.25 \times 10^{14}/cm^2$ to prevent the implanted manganese ions from diffusing from the surface of the wafer during later annealing and to keep the content of Mn at a high level near the surface. Then, sample 1 was annealed at 400°C for 30 min under flowing $N_2$ gas. Sample 3 was annealed at 800°C for 30 s under flowing $N_2$ gas. Sample 2 was not annealed.

## 3. Compositional and structural analyses

In order to investigate the distribution of Mn ions along the depth and the structure of samples, Auger electron spectroscopy (AES) and X-ray diffraction (XRD) were applied for composition and structure analyses.

### 3.1. Compositional analyses

AES was employed for analyzing the surface composition of samples and their compositional

variation along the cross section. The AES system used in this experiment is SAM PHI-610.

The AES spectra in Fig. 1 shows that there are manganese, gallium, nitride, carbon and oxygen at the sample surface. The carbon disappears inside the samples. Fig. 2 is the AES depth profile. Although the oxygen is very high at the surface, it decreases rapidly along the depth, which was introduced by oxidation of manganese after the samples were taken out of the growth chamber. The Mn atomic concentrations of sample 1 reach the maximum at the depth of 15 nm, and quickly drop down from the maximum point. Those of samples 2 and 3 reach the maximum at the depth of 45, and 60 nm, respectively, and slowly drop down. It indicates that the Mn ions reach deeper in samples with the higher substrate temperature. Post-annealing slightly affects the depth of Mn ions. The content of Mn is very high near the surface, because the manganese ions with energy of 100 eV are deposited on the surface of wafers to prevent the implanted manganese ions from diffusing from the surface of the wafer during annealing and to keep the content of Mn at a high level near the surface.

### 3.2. Structural analyses

XRD was applied for structure analyses. The XRD system used in this experiment is Philips X'pert-MRD (X'pert Materials Research Diffractometer System) with a multipurpose sample stage. The wavelength of X-ray radiated from the Cu K$\alpha$ is 0.1540562 nm.

XRD patterns of the samples were measured with $2\theta-\theta$ scan for the structural analyses. Some new reflections from oxide of Mn were found in these XRD measurements besides the diffraction peaks from GaN and $Al_2O_3$. These new reflections disappeared after the samples were etched.

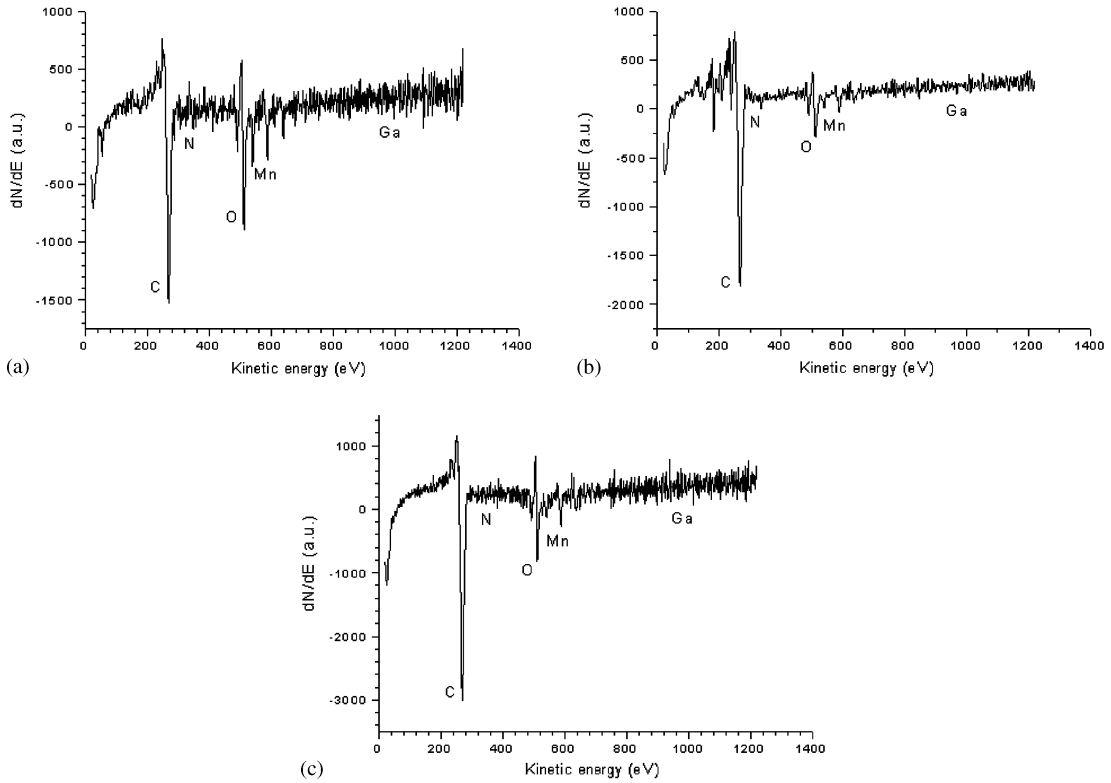


Fig. 1. Auger electron spectroscopy spectra: (a) at the surface of sample 1, (b) at the surface of sample 2, and (c) at the surface of sample 3.

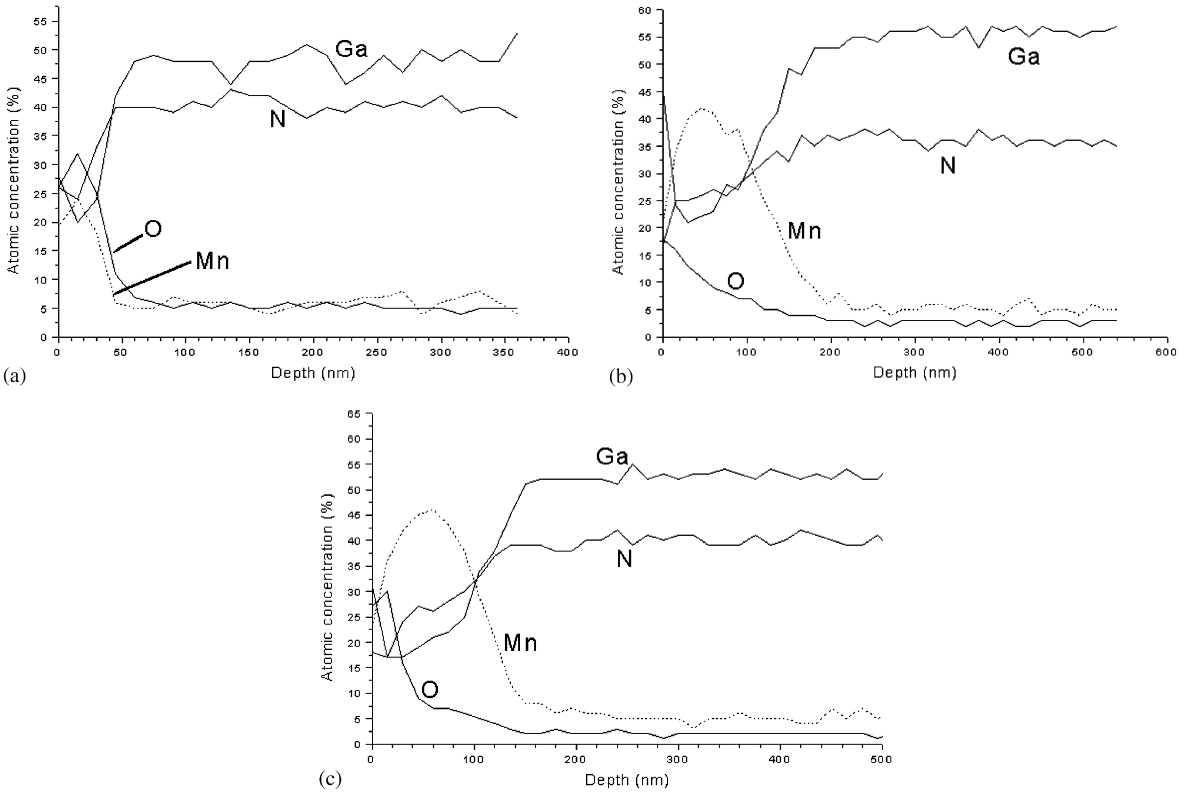


Fig. 2. Auger electron spectroscopy depth profile of: (a) sample 1, (b) sample 2, and (c) sample 3.

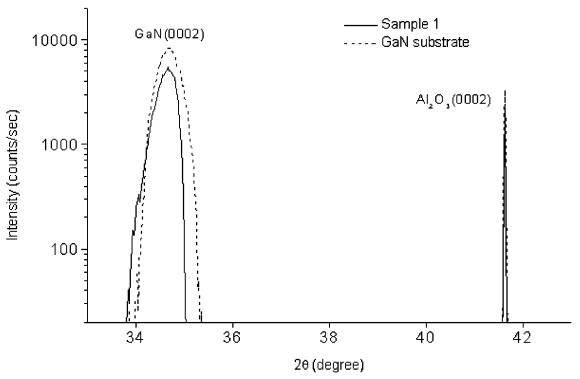


Fig. 3. X-ray diffraction pattern of sample 1.

Fig. 3 is the fine structure of the XRD pattern around (0 0 0 2) reflection from sample 1 (solid line) and GaN/$Al_2O_3$ substrate (dashed line). There is no change in the diffraction curve of $Al_2O_3$, because the implanted Mn ions do not affect the structure of $Al_2O_3$. Compared with the dashed line in Fig. 3, the GaN diffraction curve is obviously bulging to the low-angle side and the diffraction curve becomes asymmetric, but the position of the peak does not change. It indicates that $Mn^+$ ions are implanted in GaN substrate, which makes the lattice of GaN expand. New reflections are not found.

Fig. 4 is the fine structure of the XRD pattern around (0 0 0 2) reflection from sample 2. The diffraction curve of GaN/$Al_2O_3$ substrate is the dashed line. Compared with the dashed line in Fig. 4, clear diffraction peak from (Ga,Mn)N is observed and the peak difference between (Ga,Mn)N and GaN is 0.357°. Other new reflections are not found. The full-width at half-maximum of the (Ga,Mn,N) compound layer and that of the GaN substrate are 16–23 and 12–14 arcmin, respectively. It indicates that most implanted Mn atoms are incorporated in the

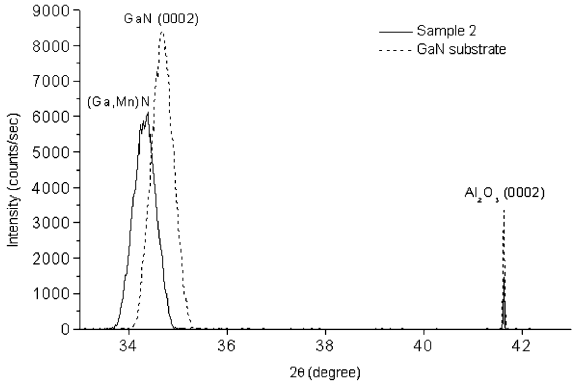


Fig. 4. X-ray diffraction pattern of sample 2.

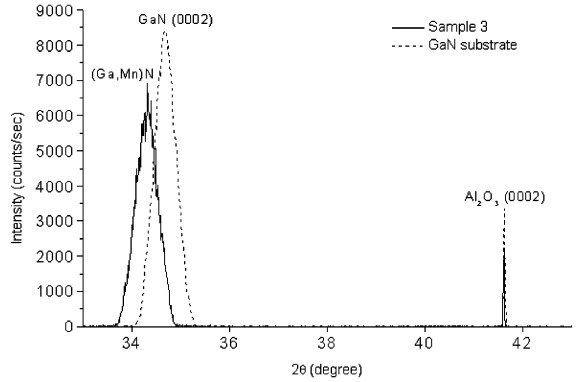


Fig. 5. X-ray diffraction pattern of sample 3.

wurtzite structure as substitutional atoms of Ga or interstitial atoms of GaN. The solid solution (Ga,Mn)N structure is formed in (Ga,Mn,N). The even lattice expansion ratio of the (Ga,Mn)N layer is calculated as 1.008% according to Fig. 4.

Fig. 5 is the fine structure of the XRD pattern around (0 0 0 2) reflection from sample 3 (solid line) and $GaN/Al_2O_3$ substrate (dashed line). Fig. 5 is very similar to Fig. 4. Clear diffraction peak from (Ga,Mn)N is observed too. The peak difference between (Ga,Mn)N and GaN is 0.377°, little bigger than that in Fig. 4. The even lattice expansion ratio of the (Ga,Mn)N layer is calculated as 1.065% according to Fig. 5. It is found by comparing Fig. 5 with Fig. 4 that high temperature annealing of sample 3 scarcely affects the structure properties. The reason is that the substrate temperatures of samples 2 and 3 are high enough, which cause the recrystallization of samples during the process of growth. So the high temperature annealing of sample 3 scarcely affects the structure properties.

## 4. Summary

The (Ga,Mn,N) compounds were obtained with mass-analyzed low energy dual ion beam deposition with Mn ion energy of 1000 eV and a dose of $2.5 \times 10^{14}\,Mn^+/cm^2$. The substrate temperature is very important in preparing samples. There is a difference between the samples grown at different substrate temperatures. The Mn ions in samples 2 and 3 grown at 400°C reach far deeper than those in sample 1 grown at 200°C. While the diffraction curve of sample 1 only is bulgy, clear diffraction peaks from (Ga,Mn)N of sample 2 and 3 are observed and this point is not reported in other papers about Mn-implanted GaN. It indicates that the solid solution (Ga,Mn)N structure is formed in our samples with the same lattice structure of GaN and bigger lattice constant. The reason why anneal of sample 3 scarcely affects the structure properties is that the energy of implanted Mn ions is low and the substrate temperature is high, which weakens the damages to crystal structure and helps recrystallization of samples during growth. No evident secondary phase formation is found in our samples.

## Acknowledgements

This work is partly sponsored by National Natural Science Foundation of China contract 60176001, the Ministry of Chinese National Science and Technology under contract PAN95-YU-34, and Special Funds for Major State Basic Research Projects G20000683 and G20000365.

## References

[1] T. Hayashi, M. Tanaka, T. Nishinaga, H. Shimada, J. Appl. Phys. 81 (1997) 4865.

[2] H. Ohno, H. Munekata, S. Molnar, L.L. Chang, J. Appl. Phys. 69 (1991) 6103.
[3] N. Karar, S. Basu, R. Venkatarghavan, B.M. Aror, J. Appl. Phys. 88 (2000) 924.
[4] H. Ohno, Science 281 (1998) 951.
[5] H. Ohno, Appl. Phys. Lett. 69 (1996) 363.
[6] N. Theodoropoulou, A.F. Hebard, Phys. Rev. Lett. 89 (2002) 107203.
[7] H. Ohno, D. Chiba, F. Matsukura, T. Omiya, E. Abe, T. Dietl, Y. Ohno, K. Ohtani, Nature 408 (2000) 944.
[8] R. Fiederling, M. Keim, G. Reuscher, W. Ossau, G. Schmidt, A. Waag, L.W. Molenkamp, Nature 402 (1999) 787.
[9] Y. Ohno, D.K. Young, B. Beschoten, F. Matsukura, H. Ohno, D.D. Awschalom, Nature 402 (1999) 790.
[10] E. Kulatov, H. Nakayama, Phys. Rev. B 66 (2002) 045203.
[11] J. Konig, H.H. Lin, A.H. MacDonald, Phys. Rev. Lett. 84 (2000) 5628.
[12] T. Diehl, H. Ohno, F. Matsukura, J. Cibert, D. Ferrand, Science 287 (2000) 1019.
[13] H. Ohno, J. Magn. Magn. Mater. 200 (1999) 110.
[14] N. Theodoropoulou, A.F. Hebard, Appl. Phys. Lett. 78 (22) (2001) 3475.
[15] Y. Shon, Y.H. Kwon, D.Y. Kim, X. Fan, D. Fu, T.W. Kang, Jpn. J. Appl. Phys. 40 (2001) 5304.